

1 **Influence of particle shape on pebble transport in a mixed sand and gravel beach during low**
2 **energy conditions: implications for nourishment projects.**

3

4 Edoardo Grottoli ¹, Duccio Bertoni ², Alessandro Pozzebon ³, Paolo Ciavola¹

5

6 ¹ Dipartimento di Fisica e Scienze della Terra, Università di Ferrara, Via G. Saragat 1, 44122

7 Ferrara, Italy.

8 ² Dipartimento di Scienze della Terra, Università di Pisa, Via S. Maria 53, 56126 Pisa, Italy.

9 ³ Dipartimento di Ingegneria dell'Informazione e Scienze Matematiche, Università di Siena, Via

10 Roma 56, 53100 Siena, Italy.

11

12 Corresponding author : grtdrd@unife.it

13

14 **Abstract:**

15 Beach nourishments using coarse-gravel sediments are becoming a frequent practice to buffer

16 coastal erosion, but usually little attention is spent on fill material characteristics. A better

17 understanding of the influence of sediment characteristics on transport is crucial to establish the best

18 compatibility of fill material with native beach sediments. Pebble transport is here investigated by

19 means of the RFID tracing technique. The main purpose of the experiment was to verify whether

20 the prevalent shapes populating the beach (disks and spheres) show a different transport under low

21 energy conditions. Tracers were injected in a small and straight portion of a mixed sand and gravel

22 beach, deploying couples of marked particles of the same size (one sphere and one disk-shaped

23 pebble on the main geomorphic elements of the beach face), in order to avoid size influence on

24 transport. Tracer recovery was undertaken 6 and 24 h after the injection and wave characteristics

25 were measured during the whole experiment duration by means of a S4 directional wave gauge.

26 After 6 h the marked pebbles already underwent significant displacement with a prevalent

27 longshore component, which became evident after 24 h. The swash zone proved to be the most
28 dynamic area of the beach. According to statistical analyses (t-tests), no significant difference
29 among the displacement of different shapes resulted, even though spheres covered longer distances
30 and resulted more dynamic than disks, thanks to their capability to roll-over in the swash zone.
31 Lately, many experiments have been carried out with marked pebbles, but this is the first time that
32 an experiment is conceived to prove how shape influences pebble transport. Disks are more subject
33 to burial and due to their higher dynamicity spheres are preferred to disks for nourishment fill
34 material. A fill material comprised of spheres is regularly responding to hydrodynamic forces and
35 can positively speed up the beach recovery after storms especially in highly dynamic systems like
36 pocket beaches, typically subjected to beach rotation processes. The results show an implication for
37 coastal managers having to choose fill sources for replenishments.

38

39 **Keywords:** Sediment transport, Particle shape, Mixed beach, Swash, Gravel nourishment, Pocket
40 beach, RFID, Tracers.

41

42 **1. Introduction**

43 During the last decades beach erosion processes have gained increasing attention in scientific and
44 public medias, because of the negative effects they exert on coastal economies. For instance, a
45 decrease in beach width would mean a loss of available space for beach resorts: this has social
46 implications for regions where the economy revolves around tourism. Erosion issues are not a
47 peculiarity of this century though. Coasts are a highly-dynamic environment, characterized by rapid
48 modifications that might have nothing to do with erosion as we are used to know it. Progradation
49 and retrogradation always existed due to natural processes that are tightly connected to factors such
50 as sea-level rise, sediment supply, accommodation space. The main causes that determined the
51 inception of the erosive state in recent decades, especially in countries around the Mediterranean
52 coastline, are instead strongly related to anthropic activities such as river dredging, river damming

53 and armoring, and reforestation (Billi and Fazzini, 2017). These factors contributed to a decreasing
54 sediment load in rivers, which ultimately resulted in a harsh reduction of available sediments
55 capable to feed the shorelines adjacent to river mouths. Consequently, beaches cannot be refilled
56 naturally as incoming sediments transported by longshore drift are scarce and often intercepted by
57 structures such as groynes, piers and breakwaters. Thus, artificial replenishments are increasingly
58 used also as a form of coastal protection (Stive et al., 2013), because they are less invasive than
59 hard protection structures. Their basic concept involves the introduction of significant sediment
60 volumes into the coastal system, which is something that is desperately needed by starved beaches
61 (French, 2001) or as an adaptation measure to future sea level rise (Dornbusch, 2017). Sand is not
62 the only type of fill, coarse sediments are also occasionally used especially where wave motion is
63 high and sand replenishments would be of short duration (López et al., 2018). Nourishment projects
64 with coarse material (i.e. gravel or shingle) started in England in small scales and occasionally
65 already in the 1950s and began to proliferate in the 1970s (Hanson et al., 2002; Moses and
66 Williams, 2008); currently they are not only used to contrast erosion on natural coarse-grained
67 beaches but also as an attempt at stabilizing originally sandy beaches (Takagi et al., 2001; Cammelli
68 et al., 2004; Kumada et al., 2010; Bertoni and Sarti, 2011; Ishikawa et al., 2012). However, an issue
69 often present is the availability of coarse material from sea-bed reservoirs, as this type of sediment
70 is only available in continental shelf seas, where large fluvioglacial deposits are available, like in
71 the North Sea. The solution is to use sediment from inland quarries or crushed fill.

72 Regarding nourishment projects made with coarse material, particle shape is an important factor to
73 consider along with grain size. The most common scheme used to describe particle shape is the one
74 proposed by Zingg (1935), which is based on particle's axis ratios., Domokos et al. (2010) recently
75 introduced a shape descriptor based on the number of static balance points of the particle. The first
76 studies attempting to explain the transport of different particle shapes date back to the 1940s and
77 1960s.. Krumbein (1942) noted already that under traction spheres move faster than any other
78 shape: this was later explained by Shephard and Young (1961) and by Kuenen (1964) as disks have

79 lower pivotability, and a lower pivotability means a lower mobility in traction (Bluck, 1967). Bluck
80 (1967) distinguished among four cross-shore facies of gravel distribution based on size and shape of
81 particles. However, the Bluck (1967) cross-shore size and shape segregation is not recognizable
82 everywhere: the clarity and number of these cross-shore facies tend to diminish when the beach
83 system is dominated by longshore transport (Carter et al., 1990a, b; Carter and Orford, 1991).
84 According to Orford et al. (2002) particle shape represents a major complicating factor in sediment
85 cross-beach differentiation. The degree of shape zonation on the beach is a function of wave energy
86 conditions and an increase of shape segregation is produced by swell wave action, depending also
87 on wave phase and breaker type (Orford, 1975). Carr et al. (1970) analyzing different shape ratios
88 and indexes concluded that c-axis (i.e. particle thickness) is the most decisive factor in determining
89 pebble sorting by wave action. Shape is also important parameter that controls the slope angle of
90 pebble stockpile due to imbrication that may occurs and can influence pebble sorting (McLean and
91 Kirk, 1969). According to Williams and Caldwell (1988), particle shape predominates when wave
92 energy condition are low, whereas size and weight influence sediment sorting when energy
93 conditions are high. Thus, a better understanding of the influence of particle shape on sediment
94 transport is crucial in nourished beaches characterized by low energy conditions. On gravel beaches
95 there is an important saltating population made by sphere-shaped pebbles when the bed is
96 dominated by disks or oblate shapes (Isla and Bujalesky, 1993). Individual clast motion is surely
97 dictated by a number of micro-mechanical factors ascribable to shape and size over a heterogeneous
98 bed (Buscombe and Masselink, 2006). Ciavola and Castiglione (2009) experimented that disk-
99 shaped pebbles in a microtidal mixed sand and gravel beach moved down towards the beach step
100 under higher wave energy and slid-up the beachface as conditions turned milder. Grottoli et al.
101 (2015) already showed some preliminary results on differential transport of pebbles according to
102 shape and size, but those findings were based on post-experiment reconstructions and not direct
103 observations as the process was taking place. As previously demonstrated, coarse sediments do
104 move under fair-weather conditions especially in the swash zone, which consequently is the area

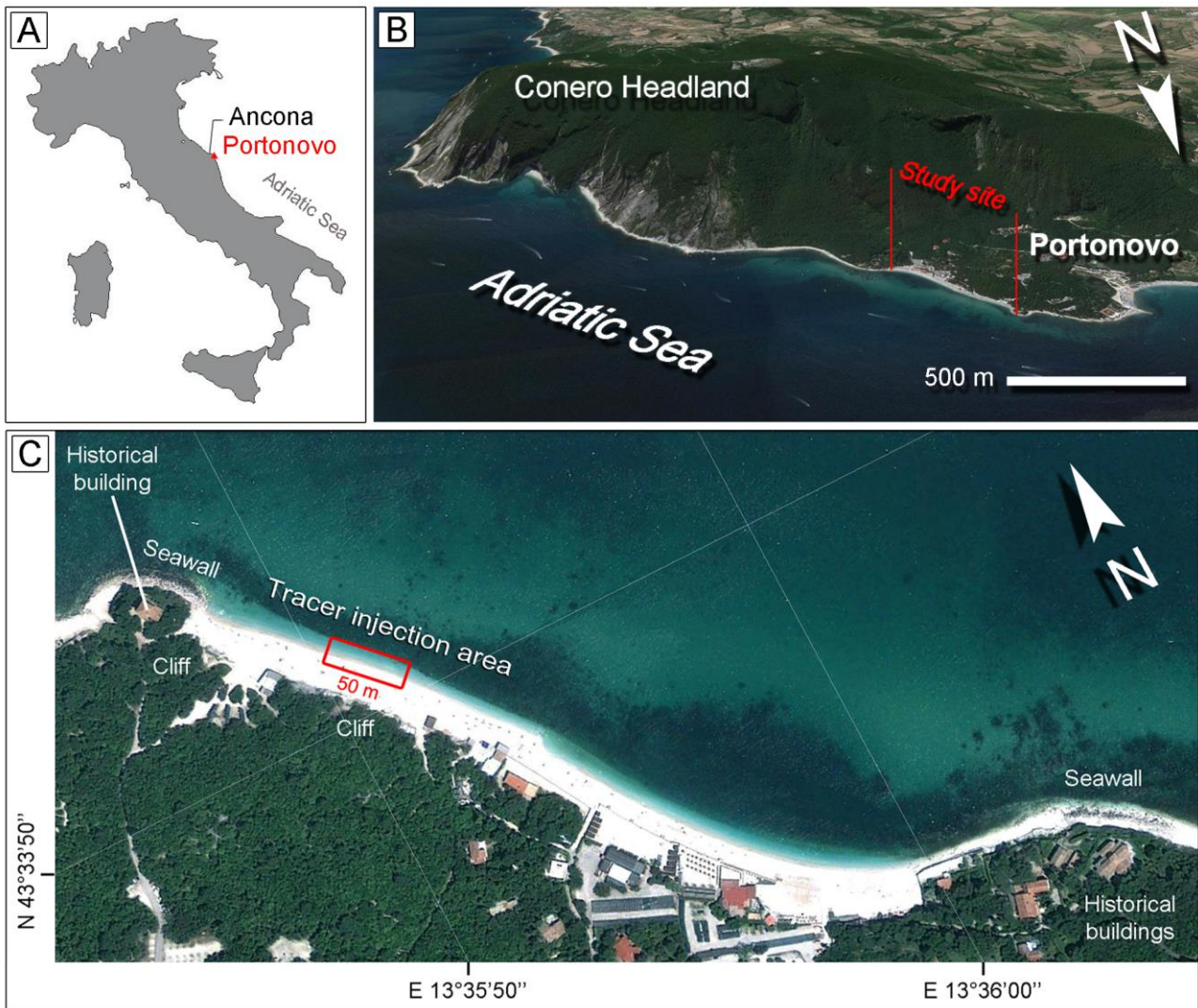
105 where sediments show the highest mobility rates also in short timespans (Bertoni et al., 2013;
106 Grottoli et al., 2015). Based on the huge mass loss reported on marked pebbles injected on artificial
107 gravel beaches (Bertoni et al., 2012; Bertoni et al., 2016), or on native coarse-grained beaches
108 (Matthews, 1983; Latham et al., 1998; Chen and Stephenson, 2015; Cox et al., 2018) the durability
109 of gravel nourishments is strongly affected by the type of filling material (Dornbusch et al., 2002).
110 In this sense, insights about the relations between particle shape and transport may be crucial in
111 supporting coastal managers making the best decisions when designing coarse sediment
112 replenishments. The aim of this paper is to improve the understanding of transport behavior (or
113 patterns) of coarse sediments in relation to their shape under low energy conditions. Implications
114 for coastal managers having to choose fill sources for gravel nourishments are found.

115

116 **2. Study area**

117 The experiment was set up on a mixed-sand-and-gravel beach (in accordance with the classification
118 of Jennings and Shulmeister, 2002) at Portonovo, a small village located in the northern part of the
119 Conero Headland (Fig.1), about 9 km southeast of the city of Ancona (central Adriatic Sea). The
120 Portonovo seaside is divided in two sectors, separated by a small armored headland; these
121 protections were built to defend an historical tower from severe damage during major storms. The
122 eastern part of the beach was selected for the experiment as it is just 500 m long (the western sector
123 is 700 m long) and delimited between two protection structures that prevent any sediment exchange
124 with the adjacent sectors, especially coarse particles. Beach width is variable (about 20 to 60 m) and
125 largely depends on the direction of storms, which eventually determine the complete rotation of the
126 beach (Grottoli et al., 2017). The prevalent grain-size is gravel, which usually piles up on the
127 backshore; the coarsest sediments accumulate on the swash zone, especially on the step. The sandy
128 fraction is mainly present in the upper portion of the backshore and offshore of the step. However,
129 as sediment redistribution after storms is high on this beach, the mutual position of each grain-size
130 is particularly dynamic. Limestones and marls mainly constitute gravel and pebbles; the sand is

131 produced by progressive disaggregation of the coarser fraction. Portonovo's beach was naturally fed
132 just by limited cliff erosion, as no rivers flow within. The erosion issues experienced in the last
133 decades along the local shores pushed local administrations to invest funds in coastal protection
134 structures (groynes, armoring), but as beach retreat would not cease, they also undertook artificial
135 replenishments to compensate for sediment loss. Almost 20000 m³ of alluvial material from inland
136 quarries were unloaded on the western side of the Portonovo seaside between 2006 and 2011;
137 unfortunately there is no record of the volume that was released on the eastern sector. The fill
138 material was constituted by pebbles and cobbles of average diameter of about 4-100 mm; textural
139 parameters and lithology were akin to those naturally present on the beach (personal
140 communication by local authority). As beach concessions occupy this sector of the coast, the
141 backshore is subjected to artificial flattening in April, in order to enlarge the beach width for the
142 summer season, a common practice on most Adriatic beaches (Harley and Ciavola, 2013). Although
143 the beach is highly anthropized, it recovers quite fast in response to forcing (Grottoli et al., 2017):
144 the beachface slope is typically 0.2, while the seafloor is about 0.01. The most intense storms are
145 northeasterlies and southeasterlies, which correspond to the dominant winds, "Bora" and "Scirocco"
146 respectively. The most typical wave height is comprised in the interval between 0.25 and 2 m. The
147 average tidal range at spring tide is 0.4 m.



148

149 Figure 1 - Portonovo study site: geographic location relative to Italy (A); local geographic location
 150 (B); Portonovo beach overlook and experiment area (C).

151

152 **3. Materials and methods.**

153 *3.1 RFID technique and tracer preparation.*

154 Tracer displacement was investigated by means of the Radio Frequency Identification (RFID)
 155 technology. This technology allows the unambiguous identification of an item by means of radio
 156 transmission. In particular, an RFID system is composed of two devices: an RFID reader, which
 157 generates an electromagnetic (EM) field that is used to interrogate, and eventually power, the
 158 second device, i.e. the transponder (or tag). The tag is the actual electronic label that is positioned
 159 on the item to be identified, i.e. the element allowing the unambiguous identification of the pebble

160 to which is coupled: it can be either passive (powered by the EM field generated by the reader) or
161 active (powered by a battery) and it is provided by an hexadecimal code and a variable amount of
162 memory (from few bytes to some tens of kB). RFID systems can operate at different frequencies,
163 ranging from Low Frequencies (LF) to Ultra High Frequencies (UHF) and microwaves. Since the
164 solution used to track the pebbles had to operate also underwater, a Low Frequency 125 kHz RFID
165 system was used: indeed, at lower frequencies the EM field is able to penetrate water for limited
166 distances. The 125 kHz RFID reader used for the experimentation proved to detect the presence of
167 tags also underwater for distances up to some tens of cm: in particular, the reader generates a
168 spherical EM field with a 40 cm radius, which represents the maximum detection range both
169 underwater and in subaerial environments. To operate underwater, an ad-hoc waterproof reader was
170 used, able to work at depths up to some meters and for prolonged periods of time, up to some hours.
171 Differently from previous solutions (Benelli et al., 2012) for this experiment the reader was
172 equipped for the first time with a Bluetooth data transmission channel able to send the code
173 retrieved by detecting a marked pebble directly to the smartphone held by the operator, thus
174 avoiding the use of a wired laptop connected to the reader. The Bluetooth transmitter was placed
175 outside the water together with the 12 V lead-acid battery powering the reader, connected to the
176 reader by an RS232 Serial cable. Once a tracer particle was detected, a message appeared directly
177 on the smartphone of the operator in charge of data collection, while an acoustic signal was also
178 emitted by the Bluetooth transmitter as an additional warning sign of pebble detection.

179 The marked pebbles were prepared by drilling a hole along the longer axis in order to have enough
180 space to accommodate the tag (cylinder glass tag with a diameter of 3 mm and a length of 22 mm,
181 Fig. 2A); the hole was sealed with a waterproof resin, resulting in a weight loss not exceeding 3 g
182 from the original weight. The size limit for sediment tracing was 24 mm, depending on the size of
183 the tag of choice. Pebbles were randomly collected from the beach surface (backshore and beach
184 face) avoiding to exceed the size limit for drilling operations and making sure to collect sediments
185 representative of the beach grain size. Spheres and disks were separated, matching those with

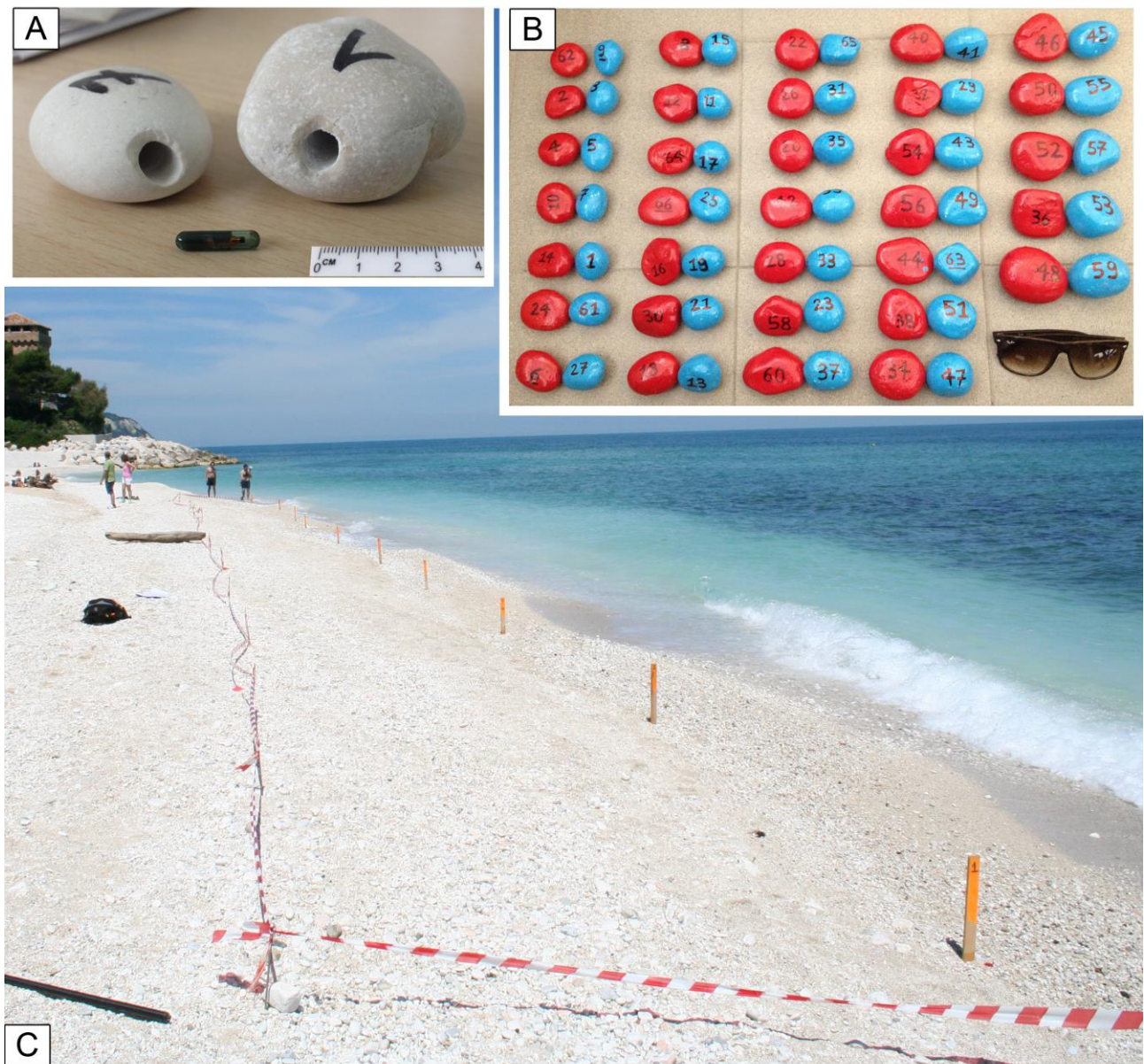
186 similar size. Once marked, tracers were painted with two different colors (red disks and blue
187 spheres, Fig. 2B) in order to make their identification easier during the short-term experiment. The
188 pebble displacements were measured recording their location by means of an RTK-DGPS (Trimble
189 R6, instrument accuracy approximately ± 3 cm). Analyses on tracer displacement were also
190 undertaken by means of statistical analyses (t-tests and box plots).

191

192 *3.2 Experiment set up*

193 The field test was set up on a central straight portion of the beach distant enough from longshore
194 protections and from the embayed shoreline typically affecting the southeastern sector (Fig. 1).
195 These factors can alter pebble displacements as experienced in previous experiments on the same
196 study site (Bertoni et al., 2013; Grottoli et al., 2015). According to Grottoli et al. (2017), Portonovo
197 beach is subjected to an intense sediment displacement after storms depending on the direction of
198 incoming waves. This process is responsible of beach rotation around a focal point, which usually
199 does not experience huge modifications. The present experiment was carried out on this sector of
200 the beach in order to reduce the influence of sediment redistribution or loss in case wave motion
201 would have increased during the time frame of the research. That was just a precaution as weather
202 forecast was carefully taken into account to avoid the concomitance of a high-energy event. At
203 10:00 am of 20th May 2014, 60 marked pebbles (30 spheres and 30 disks) were injected along 10
204 cross-shore profiles, 5 m spaced, covering a whole longshore extent of 50 m. All tracers had
205 approximately the same characteristics (weight min. 70 g, max. 188 g; mean diameter min. 39 mm,
206 max. 59 mm). Tracers were injected on the beachface of each profile as it follows: 2 tracers (1
207 sphere and 1 disk) on the fair-weather berm; 2 tracers (1 sphere and 1 disk) at the swash mid-point
208 and 2 tracers (1 sphere and 1 disk) on the beach step. As pebble shape was the only characteristic to
209 be investigated in relationship to their displacement, tracers were coupled in order to avoid large
210 difference in size and weight (Fig. 2B). Since the detection range of the RFID antenna was
211 approximately 0.4 m, only displacements greater than 0.5 m were considered significant for our

212 results. The wave characteristics were recorded using an InterOcean S4 directional wave gauge
213 during the whole experiment time. The sensor was deployed underwater few meters seaward of the
214 beachface (-1.5 m below the Mean Sea Level) for the entire experiment. Recording time of 20 min
215 per each hour with a separation of 10 min was set, measuring the water level and wave parameters
216 at a frequency of 2 Hz. RTK-GPS measurements of the 10 profiles where tracer injection took place
217 were undertaken both at the injection and at the final tracer recovery in order to record the
218 topographic variation of the experiment area.



219

220 Figure 2 - Tracers and experiment set up: drilled pebbles and tag sample (A); couples of marked
 221 pebbles with red disks and blue spheres (B); experiment beach area at 12.00 am of May 20th 2014
 222 (C).

223

224 **4. Results**

225 *4.1 Wave energy conditions.*

226 During the experiment, low energy conditions were recorded by the S4: an average value of 0.1 m
 227 of significant wave height and an average value of 6.2 s of peak wave period were registered. The
 228 wave direction was predominantly from E (Fig. 3). The maximum significant wave height value

229 (0.23 m) was registered at the very beginning of the experiment, whereas the maximum water level
230 (0 m above mean sea level) was recorded after the 6 h tracer recovery and remained stable for few
231 hours (Fig. 3). According to the computed surf scaling parameter (Battjes, 1974; Guza and Inman,
232 1975), wave breaking during the experiment occurred as surging or collapsing, which is typical on
233 reflective and steep coarse-grained beaches.

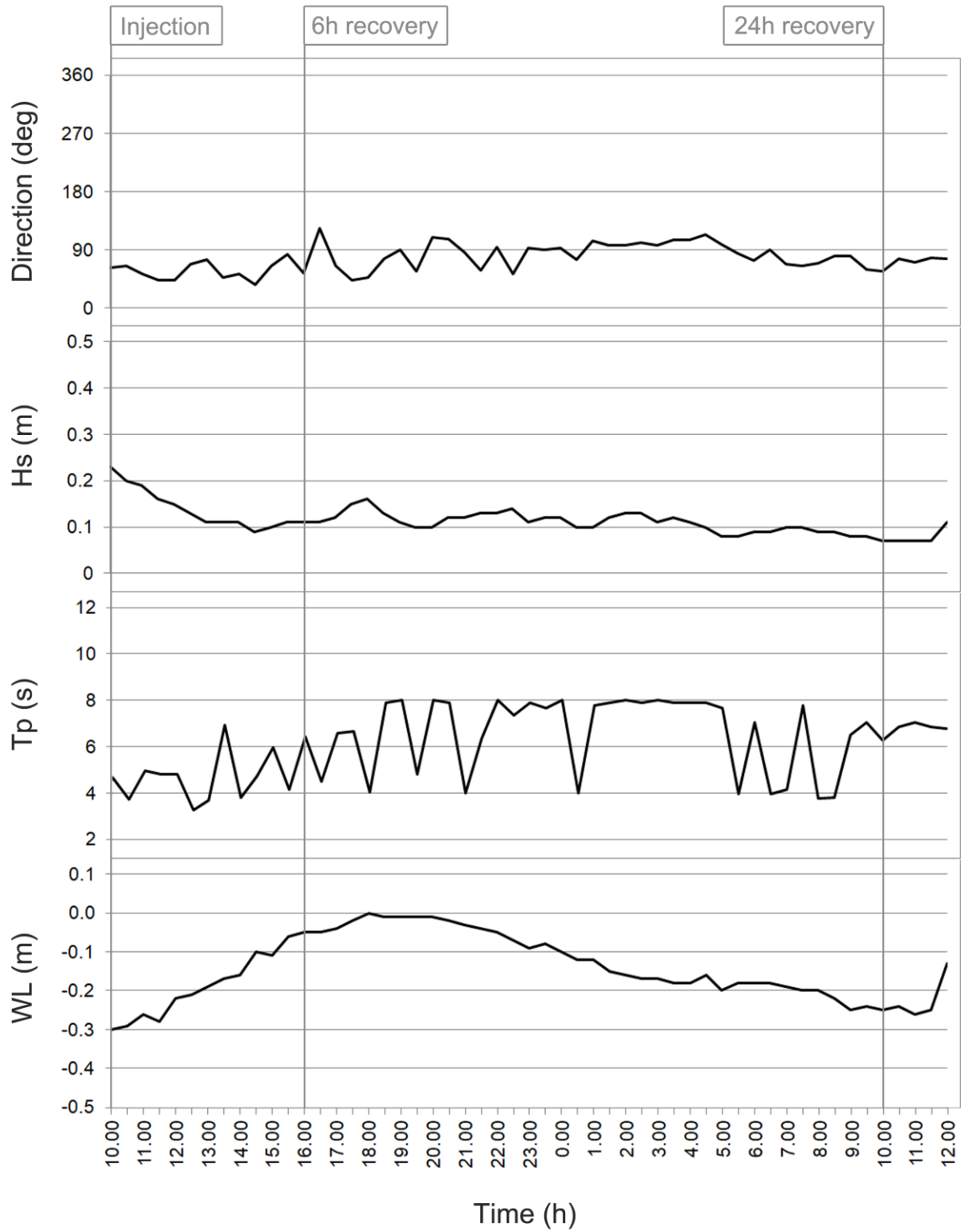
234

235 *4.2 Tracer displacement.*

236 Tracer recovery after 6 h reached 88% (93% spheres and 83% disks), but decreased to 75% after 24
237 h (80% spheres and 70% disks). Most of the tracers moved more than 0.5 m (62% of the whole)
238 after 6 h, with a maximum displacement of 19.5 m covered by a sphere-shaped pebble. After 24 h,
239 45% of the recovered tracers moved more than 0.5 m and the maximum displacement resulted 35
240 m, also this time traveled by a sphere. Considering the shape of pebbles, 63% of spheres and 60%
241 of disks moved more than 0.5 m 6 h after the injection. After one day, 57% of spheres and 33% of
242 disks moved more than 0.5 m.

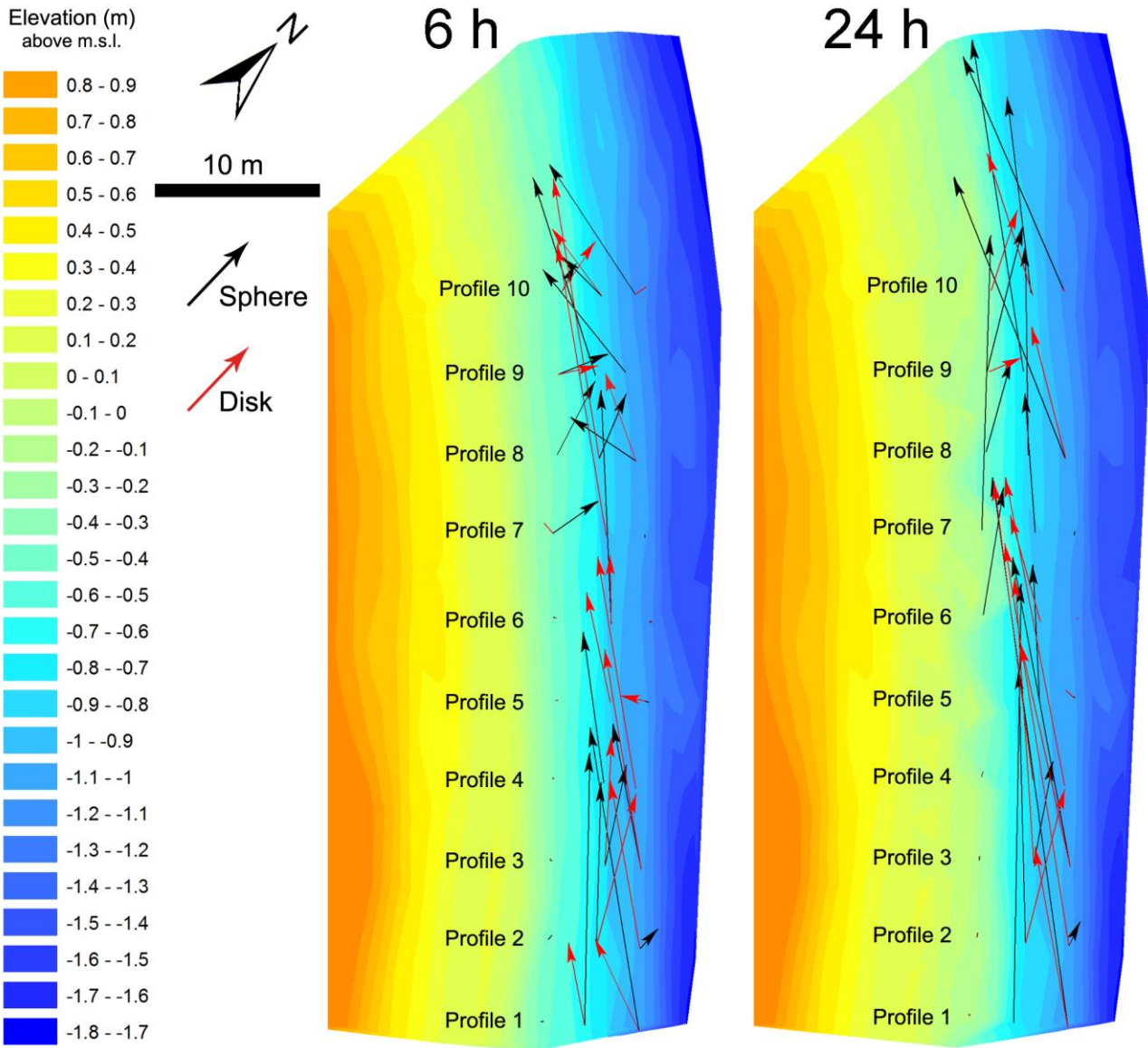
243 After 6 h most of the displaced tracers moved along the beach face with a stronger longshore
244 component, which affected in particular the tracers injected in the southeastern sector of the
245 experiment area (Fig. 4). Among the displaced tracers, those injected in the swash zone and step
246 resulted more dynamic both among spheres and disks (Fig. 4 and Fig. 5A). No tracers moved from
247 the berm to the step: as a matter of fact, considering profiles 1 to 6, berm tracers basically did not
248 move, whereas those injected in profiles 7 to 10 shifted down the beachface toward the swash zone,
249 especially among spheres (Fig. 4 and Fig. 5A). Swash tracers moved along the swash zone
250 especially among spheres, which resulted more dynamic if compared to the disks (Fig. 5A). Disk-
251 shaped step tracers moved preferentially toward the swash zone, whereas the spheres injected in the
252 step zone moved both toward the swash zone and to the fair-weather berm (Fig. 4 and Fig. 5A).
253 The longshore component of tracer transport became more evident 24 hours after the injection (Fig.
254 4). Again, the tracers injected in the step and swash zone resulted more dynamic (Fig. 4 and Fig.

255 5B) both among spheres and disks. The 50% of disk-shaped tracers injected in the swash zone was
256 not detected (Fig. 5B) and 50% of berm tracers (both among spheres and disks) did not move: those
257 tracers were placed in profiles 1 to 5. Sphere-shaped tracers injected in the swash zone did not shift
258 to any of the adjacent zones (70%, Fig. 5B), but experienced a significant displacement alongshore
259 (Fig. 4). Half of disk-shaped tracers injected in the swash zone were not detected, whereas 30% of
260 them moved alongshore in the swash zone (Fig. 4 and Fig. 5B). Sphere-shaped tracers injected in
261 the step did not show a preferential recovery zone, but resulted very dynamic as well. Half of disk-
262 shaped step tracers moved towards the swash zone, whereas the other half did not move (Fig. 4 and
263 Fig. 5B).



264

265 Figure 3 - Wave and water level conditions during the tracer experiment.



266

267 Figure 4 - Displacement map 6 and 24 h after the tracer injection according to tracer shape.

A

6h position Injection position	Spheres				Disks			
	berm	swash	step	undetected	berm	swash	step	undetected
berm	60	40	0	0	70	20	0	10
swash	20	60	10	10	40	30	10	20
step	30	20	40	10	0	60	20	20

B

24h position Injection position	Spheres				Disks			
	berm	swash	step	undetected	berm	swash	step	undetected
berm	50	30	0	20	50	20	0	30
swash	10	70	0	20	10	30	10	50
step	30	10	40	20	0	50	40	10

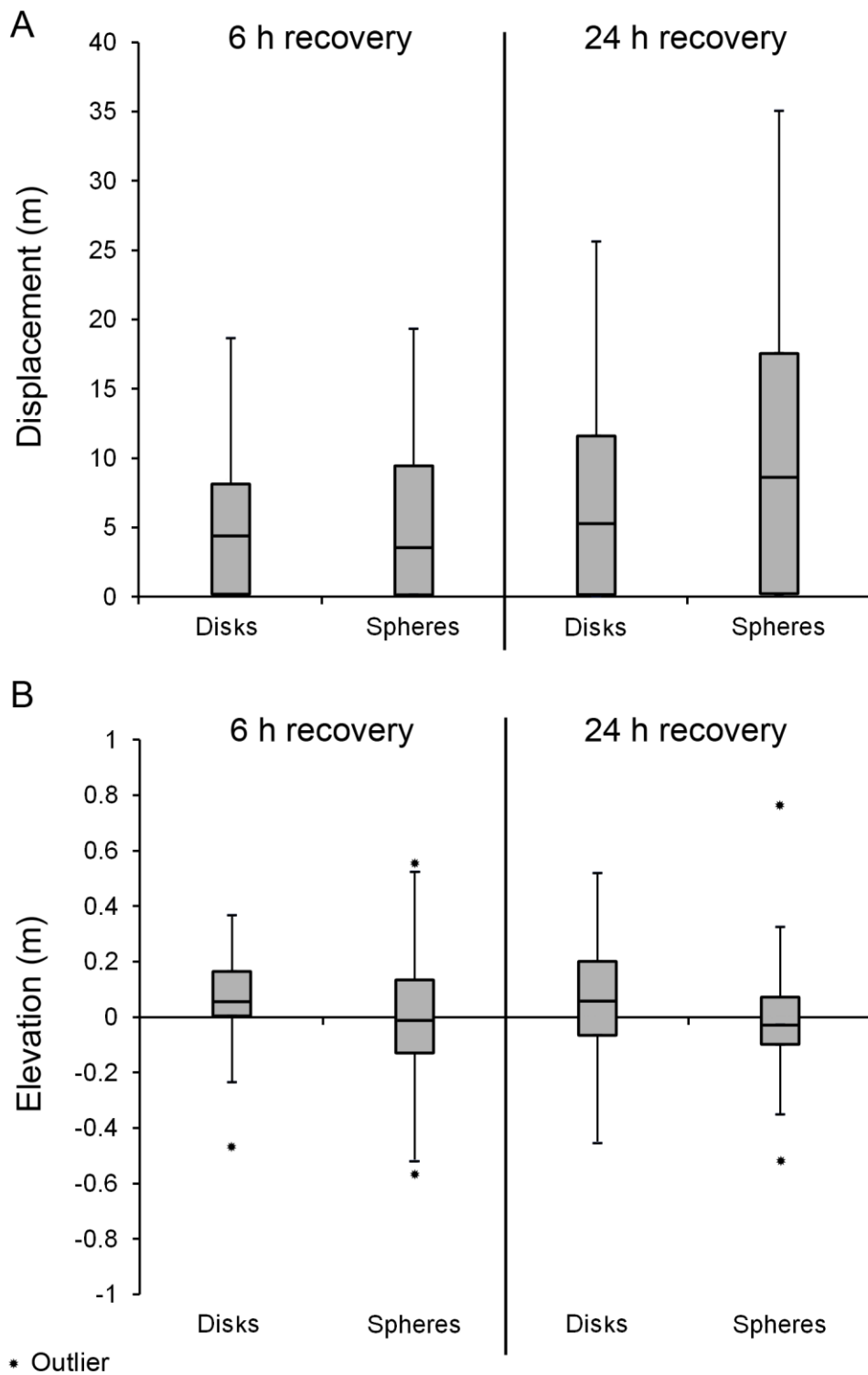
268

269 Figure 5 - Position change of spheres and disks 6 (A) and 24 (B) hours after the injection. Values
270 are given in percentage.

271

272 After 6 hours the displacement distributions of both shapes are quite similar: their distributions are
273 skewed and the median and mean displacements are around 4 m and 5.5 m respectively, with an
274 interquartile range comprised within few centimeters and 10 m. Twenty-four hours after the
275 injection sphere-shaped pebbles reached larger distances compared to disks. This is confirmed by
276 higher median and mean values (8.7 and 10.5 m respectively) and a larger interquartile range (i.e.
277 greater dispersion), which is comprised between few centimeters and 18 m (Fig. 6A and Table 1).
278 According to unpaired t-tests the difference between the displacements of spheres and disks is not
279 statistically significant since the P value, considering the two recoveries (6 and 24 h), equals to 0.96
280 and 0.24 respectively (Table 1).

281 Elevation variation among pebbles showed smaller dispersion since both disks and spheres changed
282 their elevation within ± 0.6 m during the whole experiment and always showing a symmetrical
283 distribution (Fig. 6B). After 6 h disk-shaped pebbles showed lower variation of their elevation
284 position if compared to spheres. Spheres showed the largest variation of the whole experiment
285 already after 6 h (i.e. greater interquartile range, Fig. 6B). By comparison after 24 h the disks
286 showed larger distribution and interquartile range if compared to spheres, which moved back closer
287 to the injection elevation except for two outliers. Mean values were around few centimeters for both
288 shapes, showing in both cases a mild increase in elevation compared to the 6 h recovery. Median
289 values of spheres were negative, whereas disk values were positive; mode values attested at 0 m for
290 both shapes. Again, no statistical significance resulted from t-test calculated on the elevation
291 difference between spheres and disks (Table 2).



292

293 Figure 6 - Box plots showing the displacement (A) and elevation (B) distribution of tracer recovery
 294 according to their shape.

295

296

297

Displacement	Disks (6 h)	Spheres (6 h)	Disks (24 h)	Spheres (24 h)
Mean	5.54	5.47	7.27	10.49
Median	4.38	3.56	5.34	8.68
Mode	0.84	3.51	0.07	0.22
SD	5.87	5.65	8.13	9.82
SEM	1.17	1.07	1.77	2.00
N	25	28	21	24
t-test (P value)	0.96		0.24	

298

299 Table 1 - Main statistical indexes and t-test results of the displacement distribution of the two
300 shapes: Mean, Median, Mode, Standard Deviation (SD), Standard Error of the Mean (SEM),
301 number of samples (N) and P value resulted from t-test.

302

Elevation	Disks (6 h)	Spheres (6 h)	Disks (24 h)	Spheres (24 h)
Mean	0.04	0.02	0.05	0.04
Median	0.05	-0.01	0.06	-0.02
Mode	0.01	-0.01	0.00	0.00
SD	0.21	0.29	0.26	0.30
SEM	0.04	0.05	0.05	0.06
N	25	28	21	24
t-test (P value)	0.77		0.84	

303

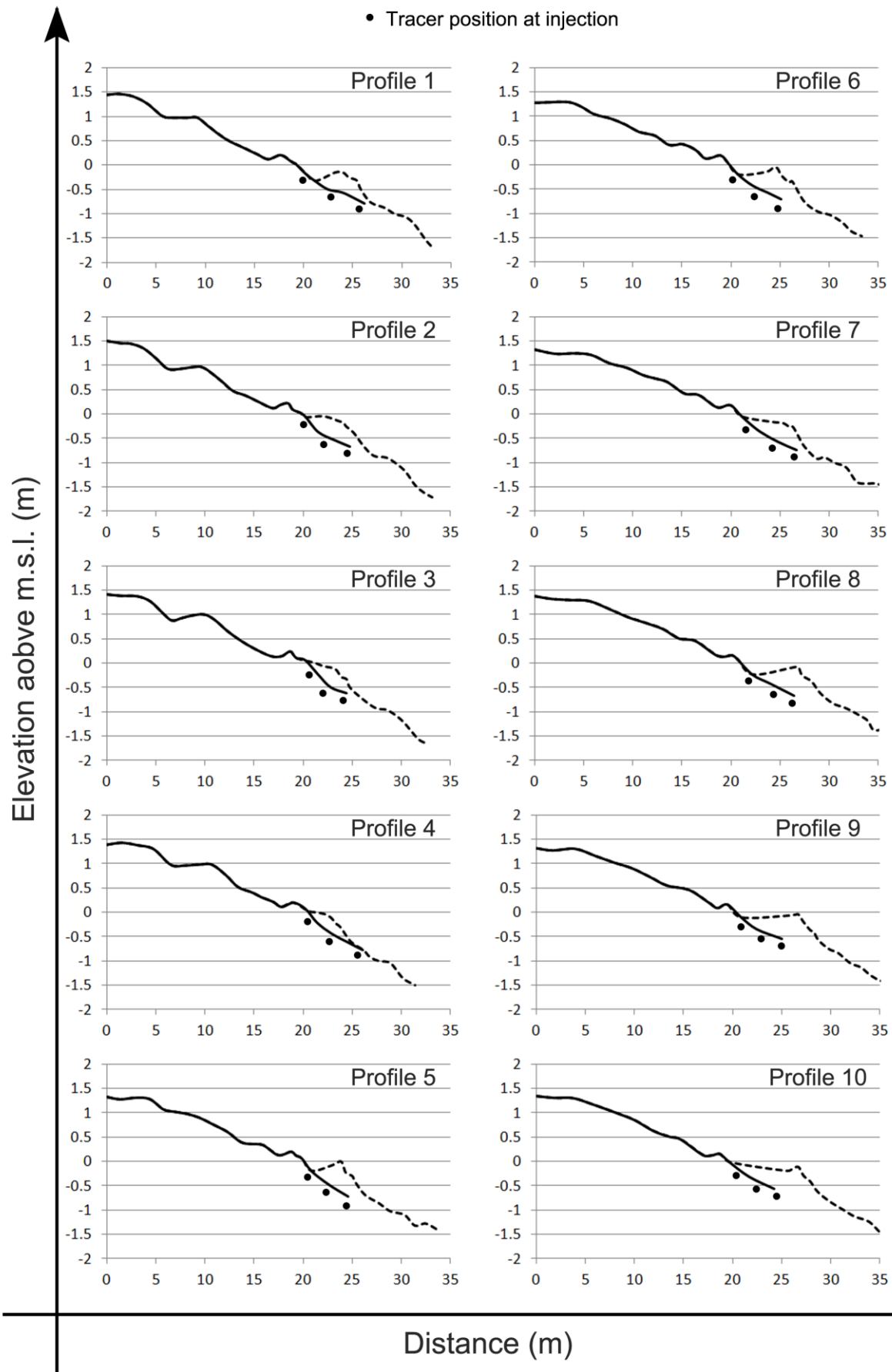
304 Table 2 - Main statistical indexes and t-test results of the elevation distribution of the two shapes:
305 Mean, Median, Mode, Standard Deviation (SD), Standard Error of the Mean (SEM) and number of
306 samples (N) and P value resulted from t-test.

307

308 *4.3 Topographic variation of the swash zone.*

309 According to topographic variation, a new fair-weather berm formed in front of the berm where the
310 tracers were injected 24 hours before (Fig. 7). An increase in elevation in the upper part of the
311 swash zone is also visible from the seaward extension of green-yellow colors of Fig. 4. The
312 maximum thickness reached by this new fair-weather berm was 0.5 m and its crest resulted more
313 distant from the one of the day before going from S to N (Fig. 7). The distance between the two
314 crests went from a minimum value of 4 m in the southeastern zone (see profiles 3 and 4) increasing
315 to a maximum of 9 m at profile 10 (Fig. 7). Furthermore, the crest of the fair-weather berm resulted
316 better developed and sharper from profile 5 to 10 (northwestern sector of the experiment area),
317 whereas resulted attached to the previous berm, without a well developed crest, at the southeastern
318 zone (especially profiles 2, 3 and 4; Fig. 7). The beachface slope was around 0.11-0.12 and did not
319 change for the whole experiment despite the formation of the new fair-weather berm.

320



322 Figure 7 - Topographic variation of the beachface between the injection situation (black continuous
323 line) and the end of the experiment (black dashed line).

324

325 **5. Discussion**

326 *5.1 Experiment considerations*

327 The prevailing longshore component affecting the tracers 6 h after the injection was not observed
328 for the majority of berm-injected tracers. Those tracers remained basically stable at the injection
329 position, especially in the first 6 profiles (Fig. 4), regardless of the shape, as they were neither
330 buried by a layer of other sediments thicker of 40 cm to result undetected nor reached,
331 entrained and displaced by swash action. This was also proved by the new fair-weather berm that
332 basically merged with that already present in profiles 2, 3 and 4 creating an armouring of sediment
333 that prevented those berm tracers from moving (Fig. 7). Swash and step tracers of those profiles
334 were largely displaced northwestwards, as they are easily reached and transported by swash
335 currents, and because of a stronger tendency to move downslope, being injected on steeper beach
336 slopes.

337 It is remarkable that 50% of disk-shaped tracers injected in the swash zone were not detected after
338 24 hours (Fig. 5B). That could be explained with the large amount of sediment deposited in the
339 northwestern part of the experiment site, also confirmed by a northwest directed longshore
340 displacement of tracers. Sedimentation in this area exceeded the 40 cm of detection range of RFID
341 antenna. Burial generated by the formation of a new fair-weather berm 50 cm high impeded the
342 recovery of some disk-shaped tracers: this could confirm the lower dynamicity of disk-shaped
343 pebbles already perceived by other authors (Shephard and Young 1961; Kuenen, 1964; Bluck,
344 1967; Grottoli et al. 2015). Likely, disks are more subjected to imbrication based on their lower
345 mobility (Bluck 1967; Orford et al., 2002; Hayes et al., 2010), and are consequently prone to burial
346 by sediments characterized by higher dynamics and regularly set into saltation like spheres (Isla and

347 Bujalesky, 1993). This process may create a protecting armouring layer (Isla, 1993) that, in the case
348 of these experiments, hindered disk recovery in the swash zone of the northwestern area.

349 As sphere-shaped pebbles need just mild forces to be displaced, they are less affected to burial
350 generated by sediments piling up. As already highlighted by Isla (1993), spheres and rounded
351 pebbles continue to overpass (i.e. capability to roll over) other sediment, usually comprised of disks
352 (Isla and Bujalesky, 1993), which are more easily trapped within the bed surface. Quite obviously
353 the swash tracers were the most dynamic ones during the experiment and this was also confirmed
354 by the topographic variations occurred on the swash zone (Fig. 7). As explained by Orford et al.
355 (2002), the lack of an effective surf zone on coarse grained beaches, due to steep angle foreshores,
356 means that hydrodynamic activity, especially on low energy beaches, is concentrated on the swash
357 zone and the actor playing the main role on sediment transport is the asymmetry of flow between
358 uprush and backwash (Kemp, 1975; Kirk, 1975; Masselink and Hughes, 1998). Despite elevation
359 variations in positioning were limited both among spheres and disks, it was interesting to realize
360 that spheres after 24 hours showed lower elevation changes, but travelled longer distances
361 compared to disks. This might also be explained with the easier capability of spheres to roll over the
362 swash zone driven by the uprush and backwash fluxes of “swash grazing” (Sherman and
363 Nordstrom, 1985), which resulted in a northwestward longshore transport being generated by
364 easterly waves. The capability to roll over the beach surface keeps the spheres always in movement,
365 whereas disks, once displaced, tend to be less dynamic and to maintain a more stable position on the
366 beach profile (Ciavola and Castiglione, 2009; Grottoli et al., 2015). This capability to roll by
367 spheres can be confirmed also by the dynamics of step tracers, since 30% of them were able to
368 climb the beachface and reach the berm position after 24 hours. On the other hand, only half of the
369 disk-shaped tracers injected on the step were able to reach the swash zone and the remaining half
370 basically did not move from the step zone (Fig. 4 and 5). This means that higher wave energy would
371 be required to slide disks up towards the berm.

372

373 *5.2 Considerations for local nourishments*

374 This study aimed at improving the understanding of the influence of pebble shape on its transport,
375 ultimately providing suggestions for a better production of fill material for nourishment projects.
376 Sediment characteristics of pebbles are very important, especially when nourishment projects,
377 contemplating coarse material, have to respect specific requirements to reproduce a fill material as
378 similar as possible to the native beach sediment. Little attention is usually spent by nourishment
379 designers on gravel shape of fill material. One should remember that shape can represent a crucial
380 characteristic: for example when natural coarse-grained beaches are highly crowded by tourists or
381 when high environmental values have to be preserved. Those requirements have surely to be
382 respected in the case of Portonovo, as the beach is part of a natural reserve and committees of local
383 beach users claiming for respecting the natural beach characteristics are currently active.
384 Consideration can be also expressed about the right choice of shape for fill material for gravel
385 nourishment both locally and elsewhere.
386 According to medium term monitoring and the proved pocket beach behavior of Portonovo
387 highlighted by Grottoli et al. (2017), it seems that there is no loss of material outside the beach
388 system. Grottoli et al. (2017) showed that consistent displacement of sediment associated to
389 shoreline rotation occur in response to storm direction but despite the high dynamicity the system
390 seems to be in equilibrium. Recent studies on native pebble transport on this beach reveals that
391 every pebble size is largely dynamic if located in the swash zone: under low energy conditions (0.2-
392 0.3 m of significant wave height) very large pebbles and cobbles (mean diameter between 48-96
393 mm), with any shape distinction, if reached by wave run-up and swash processes are mainly
394 dragged down slope towards the step zone (Bertoni et al., 2013) or are not able to slide up back to
395 the fair-weather berm if located on the step (Grottoli et al., 2015). On the other hand, smaller
396 pebbles (mean diameter between 24-48 mm) are able to “climb” the beachface and disks in
397 particular preferentially reach more stable position on the back of the fair-weather berm or at the
398 step. Spheres, being more dynamic, roll all over the swash zone continuously. Despite the high

399 dynamicity showed by Portonovo beach both under low (Bertoni et al., 2013; Grottoli et al., 2015)
400 and stormy energy conditions (Grottoli et al., 2017), the beach, being largely exposed to the effects
401 of a bimodal and opposite direction of storms (NE and SE) and being limited by defense structures
402 at its longshore edges, can quickly recover from a storm (Grottoli et al., 2017). In this perspective
403 the choice of sphere-shaped pebbles, given their higher dynamicity which is compatible to the high
404 dynamicity of the system, should be preferred for potential fill material production in the future.
405 Based on local studies produced so far, the beach in Portonovo does not seem to require any
406 sediment refill in the near future: to confirm this opinion further studies should be made on long
407 term monitoring of sediment transport coupled to analyses on abrasion rate, in order to investigate
408 how shape and size actually evolve over time through continuative high energy conditions.
409 Furthermore, as already occurred at the gravel nourished beach of Nice (Anthony et al., 2011), the
410 chance to lose material offshore has to be avoided. Being Portonovo a unique “artificial” pocket
411 beach, these considerations are very site specific: as highlighted by Sammut et al. (2017) pocket
412 beaches should be analyzed as individual coastal settings, since each beach has unique
413 characteristics related to coastal configuration, geology and exposure to incoming waves. For
414 example, Pikelj et al. (2018) on an artificial gravel beach of Croatia (Dugi Rat) highlighted
415 continuous sediment losses over 1.5 years of monitoring, despite beach re-nourishment repeated on
416 an almost yearly basis. On the other hand, the same authors noted how a natural gravel beach
417 (Brseč) rapidly responds to waves generated by the prevailing north-easterly and south-easterly
418 winds of Adriatic Sea, changing its rotation and generating sediment losses and gains.

419

420 *5.3 Consideration on fill material for gravel nourishments*

421 Hanson et al. (2002) made a comprehensive review on nourishment practices in European countries:
422 the study compares several parameters taken into account by each country for nourishment project,
423 but no mention is made about the sediment shape of fill material. The high dynamicity showed by
424 pebbles even with low energy conditions means that fill material used for gravel nourishment has to

425 be precisely defined in all its characteristics. Recent studies about pebble abrasion demonstrated
426 that the latter can be consistent, bringing to 61 % of mass loss (Bertoni et al. 2016) or 41% of
427 weight loss (Matthews, 1983) already after one year. Pebble abrasion not always depends on
428 mineral characteristics of fill material, but strongly depends on geometric aspects of pebble surface
429 leading to shape changes (Novák-Szabó et al., 2018). Gravel is usually not a popular beach material
430 because it is hard to walk on and uncomfortable for sunbathe, but fill material usually has a size
431 larger than or at least equal to the native beach sediment, so knowing how the sediment particle will
432 transform its shape and size by abrasion and transport processes is essential. In this perspective is
433 very important to better understand how gravel fill material evolves over time when deployed on a
434 native sandy beach surface. Several project have been made choosing gravel as nourishment
435 material to counteract erosion processes on native sandy beaches (Takagi et al., 2001; Cammelli et
436 al., 2004; Kumada et al., 2010; Bertoni and Sarti, 2011; Ishikawa et al., 2012), but no
437 considerations are made on shape nor shape evolution of fill material. The real issue of gravel
438 nourishment is the supply of coarse gravel (pebbles and cobbles), thus many coastal managers
439 chose to replenish using fine gravel or sand-gravel mixes (Williams, 2005; Moses and Williams,
440 2008). For this reason attempt to achieve a specific shape is not an easy task and surely could
441 represent an extra expense within the project budget. Further studies are needed to better establish
442 the lifetime of gravel nourishments in comparison with sand or mixed sand and gravel ones.
443 Understanding how coarse gravel shape can positively influence the durability of nourishments in
444 order to make this solution more sustainable is also needed since beach recharge are naturally short-
445 term fix solutions that have to be regularly repeated (Moses and Williams, 2008).

446

447 **6. Conclusions**

448 The study presents an original contribution to the understanding of the role of pebble shape on
449 controlling sediment transport in a short timespan. The transport of sphere and disk-shaped pebbles
450 was analyzed and compared as it has profound implications for the right choice of fill material for

451 gravel nourishments. Under low energy conditions all shapes move in the swash zone with a
452 predominant longshore component and remarkable displacements. Even though from this
453 experiment emerged that there is no statistical relationship between the shape of the pebbles and
454 their displacements, shape can be a discriminant factor for pebble transportation, at least under low
455 energy condition. Spheres resulted more dynamic than disks thanks to their capability to roll over
456 the swash surface. Spheres are always kept in movement by swash fluxes and taking advantage of
457 their capability to roll over the beachface can easily climb and be dragged down all over it. Disks,
458 being less dynamic, are more subject to imbrication and once displaced towards a more stable
459 position can be easily buried by other sediments. Nourishment schemes should prefer a spherical
460 shape for fill material especially on dynamic beaches (e.g. pocket beaches) where the equilibrium is
461 represented by a regular shifting of sediment in response to a bimodal wave direction.
462 Understanding how the sediment particle will transform its shape and size by abrasion and transport
463 processes is essential, especially nowadays that gravel is often preferred to sand as recharge
464 material also on native sandy shores. The precise characterization of gravel fill material is also
465 crucial given the lack of natural sources exploitable. Studies on particle shape are needed to better
466 establish the lifetime of gravel nourishments as these practices are short-term solutions that have to
467 be regularly repeated.

468

469 **Acknowledgements**

470 We want to thank professors Nancy L. Jackson and Karl F. Nordstrom for their suggestions about
471 the experiment set up and for their help during the fieldwork. Dr. Bruna Alves Rodrigues, Stefano
472 Orsetti and Silvia Di Bartolo provided crucial support during the fieldwork activities.

473

474 **References**

475 Anthony E.J., Cohen O., Sabatier F. (2011). Chronic offshore loss of nourishment on Nice
476 beach, French Riviera: A case of over-nourishment of a steep beach? *Coastal Engineering* 58,
477 374-383.

478 Battjes J.A. (1974). Surf similarity. *Proceedings 14th International Conference on Coastal*
479 *Engineering*, 466-480.

480 Benelli G., Pozzebon A., Bertoni D., Sarti G. (2012). An RFID-based toolbox for the study of
481 under- and outside-water movement of pebbles on coarse-grained beaches. *IEEE J. Sel. Top.*
482 *Appl. Earth Obs. Remote Sens.* 5:1474–1482.

483 Bertoni D., Sarti G. (2011). On the profile evolution of three artificial pebble beaches at Marina
484 di Pisa, Italy. *Geomorphology* 130, 244–254.

485 Bertoni D., Sarti G., Benelli G., Pozzebon A. (2012). In situ abrasion of marked pebbles on two
486 coarse-clastic beaches (Marina di Pisa, Italy). *Italian Journal of Geosciences* 131, 205-214.

487 Bertoni D., Grottoli E., Ciavola P., Sarti G., Benelli G., Pozzebon A. (2013). On the
488 displacement of marked pebbles on two coarse-clastic beaches during short fair-weather periods
489 (Marina di Pisa and Portonovo, Italy). *Geo-Marine Letters* 33, 463-476.

490 Bertoni D., Sarti G., Grottoli E., Ciavola P., Pozzebon A., Domokos G., Novák-Szabó T.
491 (2016). Impressive abrasion rates of marked pebbles on a coarse-clastic beach within a 13-
492 month timespan. *Marine Geology* 381, 175–180.

493 Billi P., Fazzini M. (2017). Global change and river flow in Italy. *Global and Planetary Change*
494 155, 234-246.

495 Bluck, B.J. (1967) Sedimentation of beach gravels: examples from South Wales. *Journal of*
496 *Sedimentary Petrology* 37, 128–156.

497 Buscombe D., Masselink, G. (2006). Concepts in gravel dynamics. *Earth Sci. Rev.* 79, 33–52.

498 Cammelli C., Jackson N.L., Nordstrom K.F., Pranzini E. (2006). Assessment of a gravel
499 nourishment project fronting a seawall at Marina di Pisa, Italy. *J. Coast. Res.* SI 39, 770–775.

500 Carr A.P., Gleason R., King A. (1970). Significance of pebble size and shape in sorting by
501 waves. *Sedimentary Geology* 4, 89–101.

502 Carter R.W.G., Orford J.D. (1991). The sedimentary organization and behaviour of drift-aligned
503 gravel barriers. *Coastal Sediments '91*. Am. Soc. Civ. Eng. 1, 934–948.

504 Carter R.W.G., Jennings S.C., Orford J.D. (1990a). Headland erosion by waves. *J. Coast. Res.*
505 6, 517– 529.

506 Carter R.W.G., Orford J.D., Forbes D.L., Taylor R.B. (1990b). Morphosedimentary
507 development of drumlin flank barriers with rapidly rising sea-level, Story Head, Nova Scotia.
508 *Sediment. Geol.* 69, 117– 138.

509 Chen B., Stephenson W. (2015). Measuring pebble abrasion on a mixed sand and gravel beach
510 using abrasion baskets. *Geomorphology* 248, 24–32.

511 Ciavola P., Castiglione E. (2009). Sediment dynamics of mixed sand and gravel beaches at short
512 timescales. *Journal of Coastal Research S.I.* 56, 1751-1755.

513 Cox R., Lopes W.A., Jahn K.L. (2018). Quantitative roundness analysis of coastal boulder
514 deposits. *Marine Geology* 396, 114-141.

515 Domokos G., Sipos A.Á., Szabó T., Várkonyi P.L. (2010). Pebbles, shapes and equilibria.
516 *Mathematical Geosciences* 42, 29–47.

517 Dornbusch U., Williams R., Robinson D., Moses C.A. (2002). Life expectancy of shingle
518 beaches: measuring in situ abrasion. *J. Coast. Res. Spec. Issue* 36, 249–255.

519 Dornbusch U. (2017). Design requirement for mixed sand and gravel beach defences under
520 scenarios of sea level rise. *Coastal Engineering* 124, 12-24.

521 French P.W. (2001). *Coastal Defences: Processes, Problems and Solutions*. Routledge, UK, 366
522 pp.

523 Grootjans A.P., Adema E.B., Bekker R.M., Lammerts E.J. (2008) Why Coastal Dune Slacks
524 Sustain a High Biodiversity. In: Martínez M.L., Psuty N.P. (eds) *Coastal Dunes*. Ecological
525 Studies, vol 171. Springer, Berlin, Heidelberg.

526 Grottoli E., Bertoni D., Ciavola P., Pozzebon A. (2015). Short term displacements of marked
527 pebbles in the swash zone: Focus on particle shape and size. *Marine Geology* 367, 143-158.

528 Grottoli E., Bertoni D., Ciavola P. (2017). Short- and medium-term response to storms on three
529 Mediterranean coarse-grained beaches. *Geomorphology* 295, 738-748.

530 Guza R.T., Inman D.L. (1975). Edge waves and beach cusps. *J. Geophys. Res.*, 80: 2997--3012.

531 Hanson H., Brampton A., Capobianco M., Dette H.H., Hamm L., Laustrup C., Lechuga A.,
532 Spanhoff R. (2002). Beach nourishment projects, practices, and objectives - a European
533 overview. *Coastal Engineering* 47, 81–111.

534 Harley M., Ciavola P. (2013). Managing local coastal inundation risk using real-time forecasts
535 and artificial dune placements. *Coastal Engineering* 77, 77- 90.

536 Hayes M.O., Michel J., Betenbaugh D.V. (2010). The Intermittently Exposed, Coarse-Grained
537 Gravel Beaches of Prince William Sound, Alaska: Comparison with Open-Ocean Gravel
538 Beaches. *Journal of Coastal Research* 26(1), 4-30.

539 Ishikawa T., Uda T., Miyahara S. (2012). Moving gravel body method to control downcoast
540 erosion, Proceedings of 33rd International Conference on Coastal Engineering, ASCE, 1-14.

541 Isla F.I. (1993). Overpassing and armouring phenomena on gravel beaches. *Marine Geology*
542 110, 369-376.

543 Isla F.I., Bujalesky G.G. (1993). Saltation on gravel beaches, Tierra del Fuego, Argentina. *Mar.*
544 *Geol.* 115, 263–270.

545 Jennings R., Shulmeister J. (2002). A field based classification scheme for gravel beaches.
546 *Marine Geology* 186, 211-228.

547 Kuenen (1964). Pivotability studies of sand by a shape-sorter. *Developments in Sedimentology*
548 1, 2017-215.

549 Kumada T., Uda T., Matsu-ura T., Sumiya M. (2010). Field experiment on beach nourishment
550 using gravel at Jinkoji coast. Proceedings of 32nd International Conference on Coastal
551 Engineering, ASCE, 1-13.

552 Krumbein W.C. (1942). Settling-velocity and flume-behavior of non-spherical particles.
553 Transactions, American Geophysical Union 23 (2), 621-633.

554 Latham J.P., Hoad J.P., Newton M. (1998). Abrasion of a series of tracer materials on a
555 gravel beach, Slapton Sands, Devon, UK. In: Latham, J.P. (Ed.), Advances in Aggregates
556 and Armourstone Evaluation 13. Engineering Geology Special Publications, Geological
557 Society, London, pp. 121–135.

558 López I., Aragonés L., Villacampa Y., Navarro-González F.J. (2018). Gravel beaches
559 nourishment: Modelling the equilibrium beach profile. Science of Total Environment 619-620,
560 772-783.

561 Masselink G., Hughes M.G. (1998). Field investigations of sediment transport in the swash
562 zone. Cont. Shelf Res. 19, 1179–1199.

563 Matthews E.R. (1983). Measurements of beach pebble attrition in Palliser Bay, southern North
564 Island, New Zealand. Sedimentology 30, 787-799.

565 McLean R.F., Kirk R.M. (1969). Relationships between grain size, size-sorting, and foreshore
566 slope on mixed sand-shingle beaches. N. Z. J. Geol. Geophys. 12, 138–155.

567 Moses C.A., Williams R.B.G. (2008). Artificial beach recharge: the South East England
568 experience. Z. Geomorph. N. F. 52, 107-124.

569 Novák-Szabó T., Sipos A.Á., Shaw S., Bertoni D., Pozzebon A., Grottoli E., Sarti G., Ciavola
570 P., Domokos G., Jerolmack D.J. (2018). Universal characteristics of particle shape evolution by
571 bed-load chipping. Science Advances 4, eaao4946.

572 Orford J.D. (1975). Discrimination of particle zonation on a pebble beach. Sedimentology, 22,
573 441–463.

574 Orford J.D., Forbes D.L., Jennings S.C. (2002). Organisational controls, typologies and time
575 scales of paraglacial gravel-dominated coastal systems. Geomorphology 48, 51-85.

576 Pikelj K., Ružić I., Ilić S., James M. R., Kordić B. (2018). Implementing an efficient beach
577 erosion monitoring system for coastal management in Croatia. *Ocean & Coastal Management*
578 156, 223-238.

579 Sammut S., Gauci R., Drago A., Gauci A., Azzopardi J. (2017). Pocket beach sediment: A field
580 investigation of the geodynamic processes of coarse-clastic beaches on the Maltese Islands
581 (Central Mediterranean). *Marine Geology* 387, 58-73.

582 Shepard F.P., Young R. (1961). Distinguishing between beach and dune sands. *J. Sediment.*
583 *Petrol.* 31, 196–214.

584 Sherman D.J., Nordstrom K.F. (1985). Beach scarps. *Z. Geomorphol.* 29, 139–152.

585 Stive M.J.F., de Schipper M.A., Luijendijk A.P., Aarninkhof S.G.J., van Gelder-Maas C., van
586 Thiel de Vries J.S.M., de Vries S., Henriquez M., Marx S., Ranasinghe R. (2013). New
587 Alternative to Saving Our Beaches from Sea-Level Rise: The Sand Engine. *Journal of Coastal*
588 *Research* 29, 1001-1008.

589 Takagi T., Satoh S., Yamamoto K., Sakurai W., Murano U., Atsuzaka Y., Ding Y. (2001).
590 Performance of gravel nourishment for erosion control at Fuji Coast. *Coastal Engineering* 2000,
591 3333-3344.

592 Williams A.T., Caldwell N.E. (1988). Particle size and shape in pebble-beach sedimentation.
593 *Marine Geology* 82, 199–215.

594 Zingg, T. (1935). Beitrag zur Schotteranalyse. *Schweiz. Mineral. Petrogr. Mitt.* 15, 39–140.